OPTICAL PROPERTIES AND SURFACE STRUCTURING OF $Ge_{20}Sb_5S_{75}$ AMORPHOUS CHALCOGENIDE THIN FILMS DEPOSITED BY SPIN-COATING AND VACUUM THERMAL EVAPORATION

S. Slang[1], P. Janicek[2,1], K. Palka[3,1*], L. Loghina[1], M. Vlcek[1]

[1] *Center of Materials and Nanotechnologies, Faculty of Chemical Technology, University of Pardubice, Pardubice 532 10, Czech Republic*
[2] *Institute of Applied Physics and Mathematics, Faculty of Chemical Technology, University of Pardubice, Pardubice 532 10, Czech Republic*
[3] *Department of General and Inorganic Chemistry, Faculty of Chemical Technology, University of Pardubice, Pardubice 532 10, Czech Republic*
[*] *The corresponding author e-mail: karel.palka@upce.cz*

Keywords: chalcogenide glass thin film, spin-coating, thermal evaporation, electron beam lithography, photolithography

Abstract

Thin amorphous films of $Ge_{20}Sb_5S_{75}$ composition have been deposited by spin-coating and vacuum thermal evaporation techniques. Their optical properties were investigated by spectroscopic ellipsometry in UV-NIR spectral region. We report on the comparison of thermo- and photo-induced changes in optical parameters, structure and chemical resistance of studied samples. Induced changes of films structure connected with changes of chemical stability were exploited for their surface structuring by photolithography and electron beam lithography.

Introduction

Chalcogenide glasses (ChGs) are semiconducting optical materials with high refractive index and wide IR transmission window [1, 2]. ChGs have found variety of application as material suitable for fabrication of optical elements in IR optics (e.g. fibers, planar waveguides, etc.), optical recording discs or as high resolution photoresists [1-9]. Thus, the ChGs can be used in form of bulk glass material, fibers or as a thin film deposited onto appropriate substrate [1, 2, 9].

In principle, ChG thin films can be deposited by physical vapor deposition (PVD) or solution based deposition techniques [1-14]. PVD based deposition techniques (e.g. thermal evaporation, laser ablation, etc.) are generally more developed and provide thin films of good optical quality [1, 2, 9]. PVD deposited thin films are also known for their frequent photo-sensitivity [1, 2, 16, 17].

Alternatively, ChG thin films can be deposited by solution based deposition techniques (e.g. spin-coating, dip-coating, spiral bar-coating, etc.) exploiting the fact that ChG can be dissolved in alkaline solvents, namely volatile organic amines [10-15]. Some of the main advantages of solution based deposition techniques over PVD ones are cheap instrumentation (no need for expensive high vacuum equipment) and simplicity of the thin films preparation. The solution deposited ChG thin films usually contain high concentration of organic residuals which can be reduced by post-deposition thermal treatment [10-15]. Thermal stabilization process can be challenging with respect to maintaining the films structure and elemental concentration close to the source bulk glass [12, 14]. Previous studies of solution based deposited thin films were mainly conducted on arsenic-based ChGs, which limits their widespread application due to the content of toxic arsenic [10, 11, 13]. Thus the further study

of different non-toxic ChG systems is needed in order to increase the applicability of solution based ChG thin films.

In presented work we report on the comparison of thermally evaporated and spin-coated thin films of non-toxic $Ge_{20}Sb_5S_{75}$ glass composition. The optical parameters (refractive index and optical bandgap) and morphological properties (thickness and surface roughness) of thin films were studied after different thermal and exposure treatments by spectroscopic ellipsometry. The structure and composition of as-prepared and treated thin films were studied by Raman spectroscopy and Energy-dispersive X-ray spectroscopy, respectively. Etching kinetics of studied thin films in n-butylamine based etching solution were investigated as well. Selected thin films prepared by both deposition techniques were structured using photolithography and electron beam lithography with consecutive selective etching.

Experiment details

The source chalcogenide glass (ChG) of $Ge_{20}Sb_5S_{75}$ composition was prepared by standard melt-quenching method. The high purity (5N) elements were loaded into cleaned quartz ampule and sealed under vacuum (~10^{-3} Pa). The glass synthesis was performed in rocking tube furnace at 950 °C for 72 h. The quartz ampule with melted glass was subsequently quenched in cold water.

Synthetized source bulk glass was powdered in agate bowl and quantitatively dissolved in n-butylamine (BA) with concentration of 0.075 g of glass powder per 1 ml of BA solvent resulting in clear solution without precipitate. ChG thin films were deposited in Ar atmosphere at 2000 rpm using spin-coating (SC) technique (spin-coater SC110, Best Tools) onto soda-lime glass substrates yielding thin films of good optical quality. Immediately after deposition, the thin films were stabilized by annealing at 60°C for 20 min on a hot plate (Conbrio, Czech Republic) in order to remove excess solvent. Stabilized samples are hereinafter referred as as-prepared SC thin films. The thickness of as-prepared spin-coated samples was ~390 nm.

Thin films were also deposited by vacuum thermal evaporation (TE) technique (device UP-858, Tesla corp.). The films were prepared from source ChG bulk glass by evaporation from a molybdenum boat onto soda-lime glass substrates with evaporation rate 1 nm/s at a residual pressure of ~10^{-3} Pa; the film's final thickness was ~180 nm. The thickness and evaporation rate were measured using quartz crystal microbalance method (device MSV – 1843/A MIKI – FFV). Freshly prepared samples are hereinafter referred as as-prepared TE thin films.

Thin film samples prepared by both used techniques were stored in dark dry environment at laboratory temperature.

Samples of as-prepared thin films were annealed at 110, 160 and 210 °C for 60 min on the hot plate (Conbrio, Czech Republic) in argon-filled annealing chamber. The as-prepared and annealed thin films were also subsequently exposed to the UV lamp light (main peak wavelength 365 nm, 156 $mW.cm^{-2}$) for 60 min in argon-filled exposure chamber – i.e. studied samples were exposed after their thermal treatment.

Variable angle spectroscopic ellipsometer (VASE J. A. Woollam Co.) was used for the optical properties characterization of the prepared samples. The ellipsometer was equipped with an automatic rotating analyzer over the spectral range 210 nm – 1700 nm (UV-VIS-NIR), measuring 30 revolutions with photon energy steps of 0.05 eV at three selected angles of incidence (AOI) (50°, 60° and 70°). Near normal incidence optical reflectance was measured

by the same instrument. Optical spectrometer (Shimadzu UV3600) was used for transmission spectra measurements in the spectral region 190 – 2000 nm. WVASE32 software was used for evaluation the measured data.

The etching kinetics of as-prepared, annealed and exposed thin films were studied by procedure presented in [14, 18], thin film samples were etched in 50 vol. % BA solution in aprotic solvent at 25 °C. The etching curves were evaluated at the wavelength corresponding to the interference maxima of measured transmission spectra.

The selected thin film samples (SC thin films annealed 160 and 210 °C, as-prepared TE thin films and TE films annealed at 210 °C) were exposed using contact UV photolithography (main peak wavelength 365 nm, 156 $mW.cm^{-2}$, 60 min) with exposure through chromium linear grating mask (20 μm period, ratio of the widths of exposed and shaded areas 1:1) in argon-filled exposure chamber. The thin films were subsequently etched in the etching solution (50 vol. % BA solution in aprotic solvent).

The SEM scans, electron beam lithography (EBL) exposure and elemental concentration of studied samples were obtained using scanning electron microscope LYRA 3 (Tescan) equipped with EDS analyzer AZtec X-Max 20 (Oxford Instruments). The EDS measurement was performed at 5 kV acceleration voltage. The EBL exposure of selected thin film samples (SC and TE thin films annealed at 210°C) was carried out with exposure doses 100-2500 $\mu C.cm^{-2}$. The latent images of test dose patterns and 5 μm period linear gratings were recorded and the thin film samples were subsequently etched in BA based etching solution (50 vol. % BA solution in aprotic solvent).

Surface topography of prepared grating samples was studied by atomic force microscopy method (Solver NEXT, NT-MDT) in semicontact mode. The structure of source bulk glass and studied unexposed and exposed thin films prepared by both deposition techniques was determined using FT-IR spectrometer IFS55 with Raman module FRA106 (Bruker) using excitation by Nd:YAG laser (1064 nm). The thin film samples were scrapped off into powder sample holders before measurement to increase the volume of studied material and subsequently increase the Raman signal intensity with better signal to noise ratio. The Raman spectra were measured with laser beam intensity of 200 mW (2 cm^{-1} resolution, 200 scans) and normalized by intensity of the most intense band in the spectrum.

Results and discussion

SC and TE thin films deposited onto soda-lime glass substrates were studied using spectroscopic ellipsometry. Geometrical and optical parameters were calculated via regression analysis, where minimization procedure was conducted using the mean square error (MSE) values. The sample model used for spectra analysis consists of 1) a semi-infinite glass substrate (with optical constants obtained previously on a blank sample of uncoated microscopic soda-lime glass slide), 2) a homogenous, isotropic film representing the SC and TE unexposed and exposed $Ge_{20}Sb_5S_{75}$ thin film annealed at different temperatures, 3) surface roughness modeled by a Bruggeman type effective medium approximation of the voids and layers [19], and 4) air as the ambient medium. The short wavelength absorption edge is present in the UV-VIS-NIR part of the spectra of amorphous semiconductors. Tauc-Lorentz oscillator has been used for description of this band edge of studied films [20]. In order to ensure validity of short wavelength absorption edge determination and thickness of the thin film, data from transmission and reflection have been used in the fit together with the ellipsometry data and

calculated using MSE minimization (MSE less than 4.9 for all samples). Obtained data are presented in Table 1.

Table 1. Values of thin film's thickness, surface roughness, refractive index at 1550 nm (n_{1550}) and optical bandgap (E_g^{opt}) of $Ge_{20}Sb_5S_{75}$ thin films determined by spectroscopic ellipsometry.

SC thin films				
Sample	Thickness (nm) unexp. / exp.	Roughness (nm) unexp. / exp.	n_{1550} unexp. / exp.	E_g^{opt} (eV) unexp. / exp.
as-prepared	388 / 373 ± 0.2 / ± 0.2	0.5 / 4.0 ± 0.1 / ± 0.1	1.74 / 1.70	2.34 / 2.32
T-110 °C	359 / 355 ± 0.2 / ± 0.4	1.0 / 3.2 ± 0.1 / ± 0.2	1.75 / 1.72	2.42 / 2.52
T-160 °C	260 / 257 ± 0.2 / ± 0.6	5.4 / 8.3 ± 0.1 / ± 0.4	1.86 / 1.81	2.62 / 2.66
T-210 °C	192 / 200 ± 0.1 / ± 0.1	7.9 / 9.8 ± 0.1 / ± 0.1	2.01 / 1.99	2.63 / 2.63
TE thin films				
Sample	Thickness (nm) unexp. / exp.	Roughness (nm) unexp. / exp.	n_{1550} unexp. / exp.	E_g^{opt} (eV) unexp. / exp.
as-prepared	175 / 184 ± 0.2 / ± 0.2	4.2 / 3.7 ± 0.1 / ± 0.1	2.11 / 2.05	2.61 / 2.79
T-110 °C	174 / 177 ± 0.2 / ± 0.2	3.8 / 4.7 ± 0.1 / ± 0.1	2.10 / 2.06	2.65 / 2.76
T-160 °C	169 / 178 ± 0.2 / ± 0.2	10.3 / 3.9 ± 0.1 / ± 0.1	2.09 / 2.05	2.65 / 2.74
T-210 °C	169 / 179 ± 0.1 / ± 0.1	5.6 / 5.5 ± 0.1 / ± 0.1	2.10 / 2.05	2.72 / 2.74

Previous study confirmed [14] that annealing of Ge-S based as-prepared SC thin films at temperatures above 100 °C is connected with decomposition of alkyl ammonium germanium sulfide (AAGS) salts, which were already formed in glass solution during dissolution of chalcogenide bulk glass [12]. Moreover, the spin-coated thin films of Ge-Sb-S system are nano-porous with cavities closed on the film surface [12]. The thermal decomposition of AAGS salts in film matrix is followed by releasing of organic residuals and structural polymerization resulting in more compact thin film [14]. The thickness and roughness of studied $Ge_{20}Sb_5S_{75}$ thin films are graphically presented in Figure 1. The significant thickness decrease of SC thin films with increasing annealing temperature (especially during annealing above 110 °C) can be observed on studied Ge-Sb-S thin film composition. The thickness decrease is also accompanied by increase in SC film roughness, which varies from 0.5 nm for as-prepared thin film to 7.9 nm for thin film annealed at 210 °C. The UV lamp light exposure of studied thin films was performed after their thermal treatment. The evaluated data proved that UV exposure of as-prepared SC thin film induces structural changes resulting in minor film thickness decrease and increase in film roughness. The thickness of annealed thin films seems unaffected by UV exposure, but roughness is also slightly increasing. Roughness increase of UV exposed SC thin films can be explained by potential surface photo-oxidation due to the sensitivity of spin-coated thin films to UV induced oxidation [21] and possible minor oxygen contamination of used inert argon atmosphere.

Contrary, the thickness of TE thin films is not significantly changing during annealing. Observed changes in their thickness can be probably attributed to the sample-to-sample thickness variation due to the non-ideality of evaporation process, which comes from construction of evaporator. The presented data proved increase in films thickness after UV exposure suggesting their tendency to photo-expansion. The roughness of TE thin films also slightly increased with increasing annealing temperature, but the effect of UV exposure on their values is almost negligible.

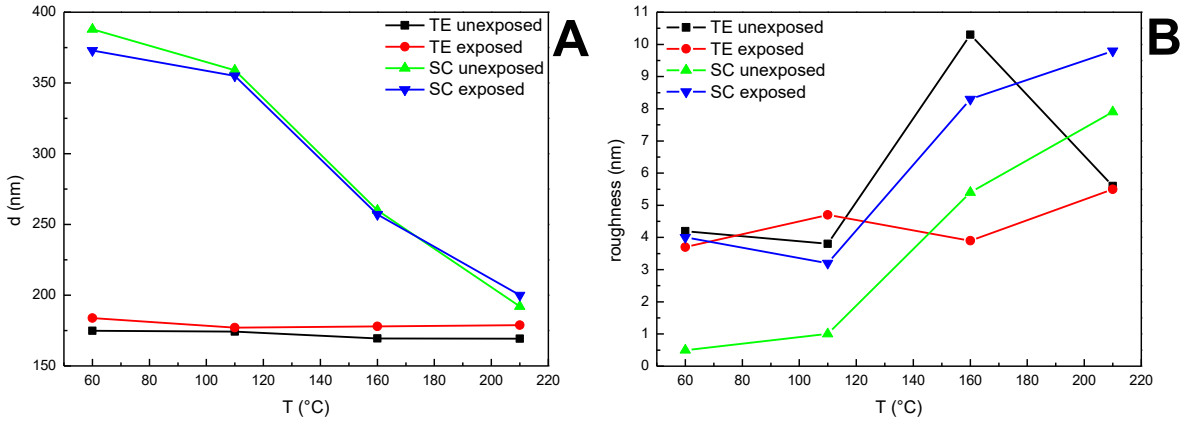

Fig. 1. The thickness (A) and roughness (B) of studied spin-coated (SC) a thermally evaporated (TE) of $Ge_{20}Sb_5S_{75}$ thin films obtained by spectroscopic ellipsometry in dependence on annealing temperature.

The refractive index of SC $Ge_{20}Sb_5S_{75}$ thin films is gradually increasing with increasing annealing temperature (Figure 2), probably due to structural changes connected with releasing of low-index organic residuals and closing of porous structure [12-15]. Contrary, the refractive index of $Ge_{20}Sb_5S_{75}$ TE thin films is not significantly changed after their annealing. It should be noted, that the majority of thermally induced structural changes of TE thin films occur at temperatures close to the T_g of annealed material [1, 2, 22]. In our experiment, the maximum annealing temperature 210 °C is still well below the T_g values of ChG with similar glass compositions [12, 23] and thus negligible changes in refractive index of prepared TE samples are understandable. The obtained data proved that both, SC and TE thin films of $Ge_{20}Sb_5S_{75}$ glass composition are photo-sensitive, as their refractive index is decreased after UV light exposure. The origin of their photo-sensitivity can be explained by UV exposure induced structural changes which are studied later in this work.

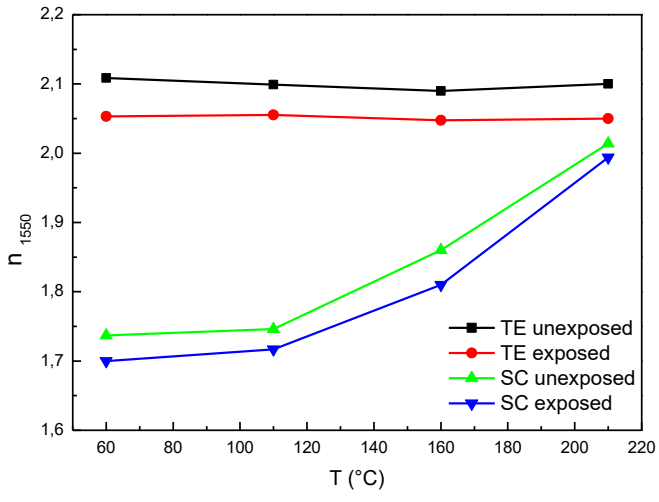

Fig. 2. The refractive index of studied spin-coated (SC) a thermally evaporated (TE) $Ge_{20}Sb_5S_{75}$ thin films obtained from spectroscopic ellipsometry in dependence on annealing temperature.

The obtained data proved the tendency of SC and TE thin films to annealing induced bleaching (blue shift), but the effect of UV exposure significantly differs between SC and TE $Ge_{20}Sb_5S_{75}$ thin films (Figure 3). The optical bandgaps of TE thin films increase after exposure (photo-bleaching), but the magnitude of photo-bleaching gradually decreases with increasing temperature of pre-exposed sample. This fact confirms higher sensitivity of studied TE samples to exposure than to annealing, as was previously observed on thermo- and photo-induced changes of refractive index values (Figure 2). It also confirms, that annealing up to 210 °C induces structural changes resulting in less photo-sensitive material.

The optical bandgap of SC thin films slightly decreases (photo-darkening) after exposure of as-prepared sample, but significantly increases (photo-bleaching) after exposure of samples annealed at 110 and 160 °C. No changes of optical bandgap were observed on thin films annealed at 210 °C.

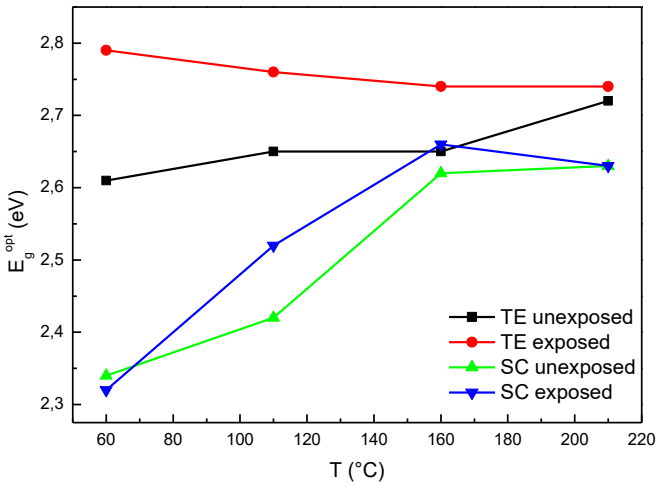

Fig. 3. The optical bandgaps (E_g^{opt}) of studied spin-coated (SC) a thermally evaporated (TE) $Ge_{20}Sb_5S_{75}$ thin films obtained from spectroscopic ellipsometry in dependence on annealing temperature.

The elemental concentration of studied samples in dependence on treatment was studied using EDS analysis. Measured composition of as-prepared TE thin film was $Ge_{21.0}Sb_{6.5}S_{72.5}$, which slightly differs from planned $Ge_{20}Sb_5S_{75}$ composition. The difference between the planned glass composition and as-prepared TE thin film can be attributed to the non-ideality of evaporation process when partial fractionation can be expected [24-25]. The EDS data proved that $Ge_{21.0}Sb_{6.5}S_{72.5}$ TE thin film composition was not changed after annealing or UV exposure. In contrast, the composition of SC thin films is changing significantly during annealing and also during UV exposure (Figure 4). The as-prepared thin film contains high concentration of N and O. The origin of N atoms can be attributed to the presence of residual BA molecules, either in form of AAGS salt molecules or as included free molecules in cavities inside film matrix [12, 14]. The oxygen atoms presence can be explained by partial film oxidation during spin-coating or thermal stabilization process. The organic residuals are gradually released with increasing annealing temperature, which can be observed in decreasing content of N and O atoms. The Ge and Sb content is also slightly decreasing with increasing annealing temperature

suggesting their evaporation probably in form of oxides [26] or oxygen containing organic compounds. The UV exposure of low temperature annealed SC thin films induces massive changes in S and O content. The samples are readily oxidized by O containing contaminant molecules (adsorbed oxygen, OH groups and/or moisture) and S atoms are released from thin film matrix. The UV irradiation induces formation of O*, OH* and Ge* reactive radicals which readily form new bonds and influence the elemental composition of UV exposed thin film [27, 28]. With increasing annealing temperature, more compact and organic residuals free films are obtained and the effect of UV exposure on elemental concentration is less pronounced. Exposure induced sulfur depletion of spin-coated $Ge_{23}Sb_7S_{70}$ thin films was also confirmed by Waldman at al. [12].

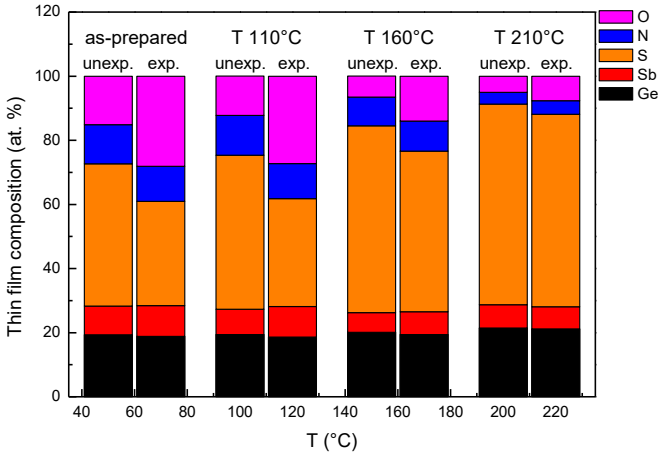

Fig. 4. The elemental concentration of studied spin-coated $Ge_{20}Sb_5S_{75}$ thin films obtained from EDS analysis in dependence on annealing temperature. The carbon content was excluded from evaluation.

The structure of $Ge_{20}Sb_5S_{75}$ thin film samples and source bulk glass was studied by Raman spectroscopy (Figures 5, 6). The samples annealed at elevated temperatures (160 and 210 °C) exhibit luminescence background in measured Raman spectra. The intensity of luminescence significantly overlaps the intensity of Raman signal in case of sample annealed at 210 °C and thus makes data non-evaluable. The main structural units of source bulk glass are corner-shared $GeS_{4/2}$ tetrahedral units with band at 340 cm^{-1} [29-32]. The additional two weaker bands at 368 and 436 cm^{-1} can be attributed to the vibration of edge-shared $GeS_{4/2}$ tetrahedral units [30, 31]. The broad shoulder at 300 cm^{-1} belong to the vibration of $SbS_{3/2}$ pyramidal units [33-35]. Due to the high overstoichiometry of sulfur, the three sharp bands of S_8 rings situated at 151, 218 and 475 cm^{-1} can be found in measured Raman spectrum [36-38]. The band of S-S vibrations at 495 cm^{-1} [36-38] should be also present in Raman spectrum, but it is almost imperceptible due to the high intensity of neighboring S_8 band at 475 cm^{-1}.

The structure of as-prepared $Ge_{20}Sb_5S_{75}$ TE thin film is very similar to the structure of source bulk glass (Figure 5). The main difference is higher intensity of S_8 rings bands (475 cm^{-1}) and bands of edge-shared $GeS_{4/2}$ tetrahedral units (368 and 436 cm^{-1}). The annealing induces only minor structural changes connected with slight intensity decrease of mentioned bands suggesting increase in ordering of films structure. The UV exposure of thin film samples induces structural changes almost identical to the annealing at elevated temperatures, but all spectra additionally exhibit higher luminescence background.

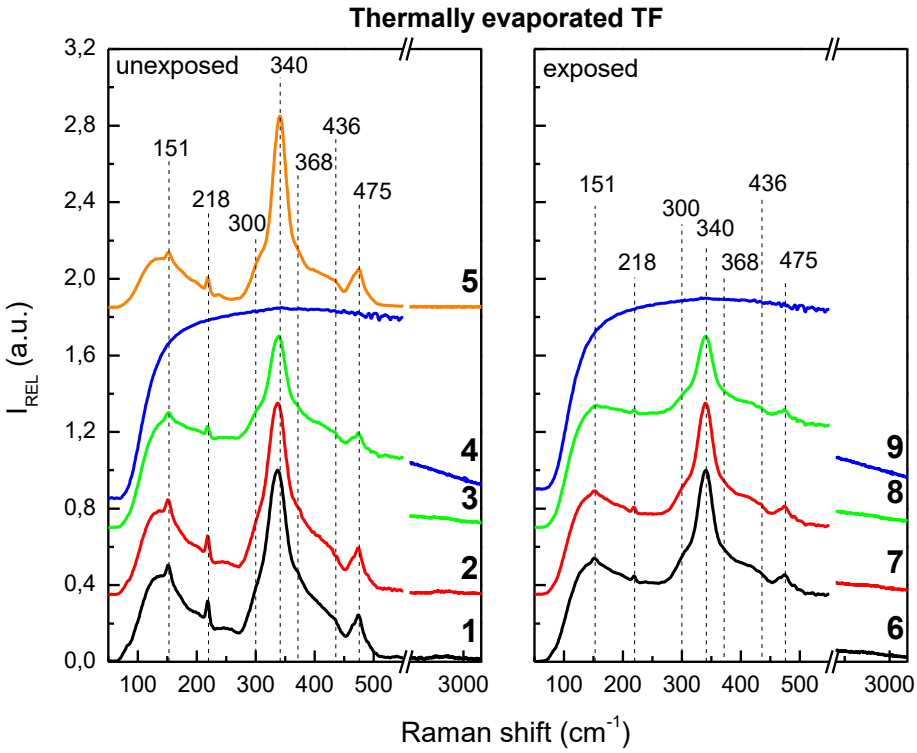

Fig. 5. The Raman spectra of TE thin films and source bulk glass of $Ge_{20}Sb_5S_{75}$ composition. 1 – as-prepared thin film, 2 – annealed at 110 °C, 3 – annealed at 160 °C, 4 – annealed at 210 °C, 5 – source bulk glass, 6 – exposed as-prepared thin film, 7 – annealed at 110 °C exposed, 8 – annealed at 160 °C exposed, 9 – annealed at 210 °C exposed.

Contrary, the structure of as-prepared $Ge_{20}Sb_5S_{75}$ SC thin films is very different from the structure of source bulk glass (Figure 6). The main structural units of as-prepared sample are also corner-shared $GeS_{4/2}$ tetrahedral units with band at 340 cm^{-1}, but their band is very sharp. The bands of edge-shared $GeS_{4/2}$ tetrahedral units at 368 and 436 cm^{-1} have a very low intensity, suggesting low level of structural polymerization. The band intensity of S_8 rings (151, 218 and 475 cm^{-1}) is much higher than in the Raman spectrum of source bulk glass and the Raman band of $SbS_{3/2}$ pyramidal units around 300 cm^{-1} is significantly wider. Three additional bands in 50-500 cm^{-1} region situated at 144, 191 and 455 cm^{-1} were also reported in Raman spectra of SC $Ge_{25}S_{75}$ thin films and they were assigned to the vibrations of organic residuals (namely AAGS salts) in thin film matrix [14]. The presence of bands at 2800-3000 cm^{-1} also confirms that structure of as-prepared SC thin film contains organic molecules [13, 14]. The annealing induced structural polymerization connected with decomposition of AAGS salts and releasing of organic residuals can be deduced from measured Raman spectra. With increasing annealing temperature, the content of S_8 rings and organic molecules decreases, the band of corner-shared $GeS_{4/2}$ tetrahedral units widens and the bands of edge-shared $GeS_{4/2}$ tetrahedral units appear in Raman spectra as a result of polymerization process.

The UV exposure of as-prepared SC sample induces significant structural decomposition. The intensity of S_8 rings vibrations increases as intensities of corner-shared $GeS_{4/2}$ tetrahedral units and AAGS salts vibration proportionally decrease. Observed phenomenon is probably connected with content of AAGS salts and oxygen contamination as the tendency of Ge-Ga-S and Ge-Sb-S thin films to oxygen assisted UV light photo-induced changes was already reported [27, 28]. Although the characteristic Ge-O-Ge vibrations at 750-900 cm^{-1} [28] were not found in measured Raman spectra, the presence of oxygen compounds in thin film matrix cannot be excluded due to the elevated oxygen content measured by EDS. The structural effect

of UV exposure gradually decreases with increasing annealing temperature of pre-exposed samples due to the increasing in their compactness (densification) and structural polymerization. It should be noted that observed photo-induced structural changes of SC samples are different from TE samples and this difference can explain different photo-induced changes of optical parameters.

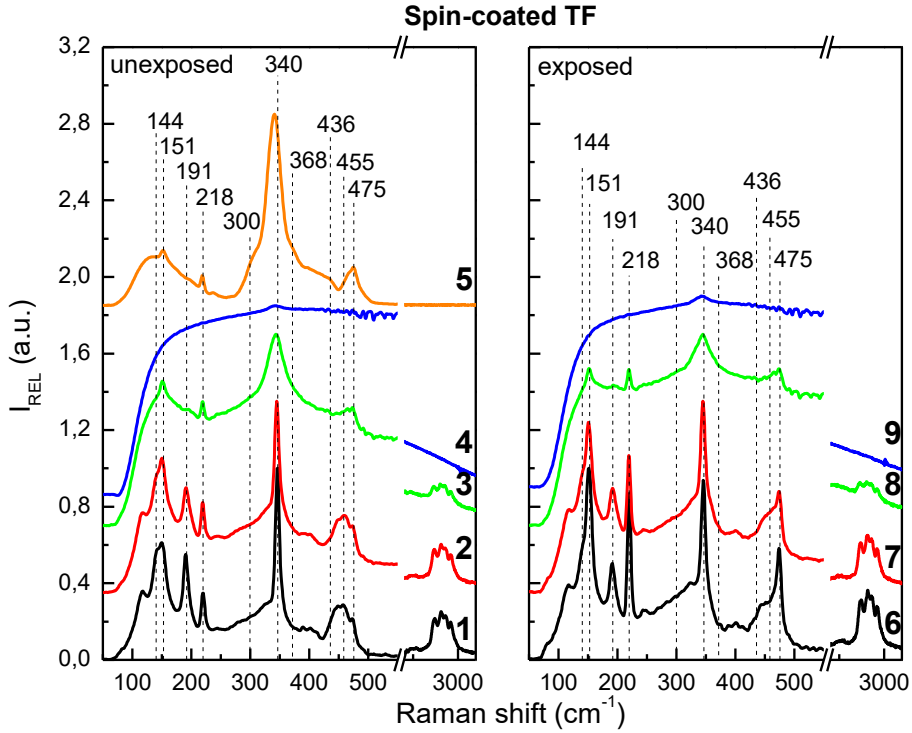

Fig. 6. The Raman spectra of SC thin films and source bulk glass of $Ge_{20}Sb_5S_{75}$ composition. 1 – as-prepared thin film, 2 – annealed at 110 °C, 3 – annealed at 160 °C, 4 – annealed at 210 °C, 5 – source bulk glass, 6 – exposed as-prepared thin film, 7 – annealed at 110 °C exposed, 8 – annealed at 160 °C exposed, 9 – annealed at 210 °C exposed.

In order to study the effect of annealing and exposure on chemical resistance of TE and SC thin films, the $Ge_{20}Sb_5S_{75}$ samples were etched in BA based solution using the experimental setup described in [14, 18]. Based on the obtained data of films thicknesses and etching times, the etching rates v_{etch} and etching selectivity (ratio between the etching rate of exposed and un-exposed thin film) were calculated (Figure 7). As-prepared SC samples were dissolved immediately after their immersion into etching solution and thus they are not presented in our results. Both, the TE and SC thin films increase their chemical stability (etching rate v decreases) with increasing annealing temperature. This effect is even more eminent on SC thin films due to the content of organic residuals which significantly decreases their chemical stability. UV exposure induced structural changes are also resulting in changes of films chemical stability. The annealing temperature additionally affected the etching selectivity as well. The as-prepared TE sample and SC sample annealed at 110 °C are etched faster that their UV exposed counterparts (negative etching). With increasing annealing temperature, the difference between etching rates of unexposed and exposed samples decreases and eventually the selectivity is inversed. The SC and TE thin films annealed at 210 °C are etched slower than exposed samples (positive etching). The SC thin films exhibit higher selectivity than TE thin films annealed at the same temperature but due to the absence of their luminescence-free Raman spectra, the observed effect cannot be sufficiently explained by Raman spectroscopy.

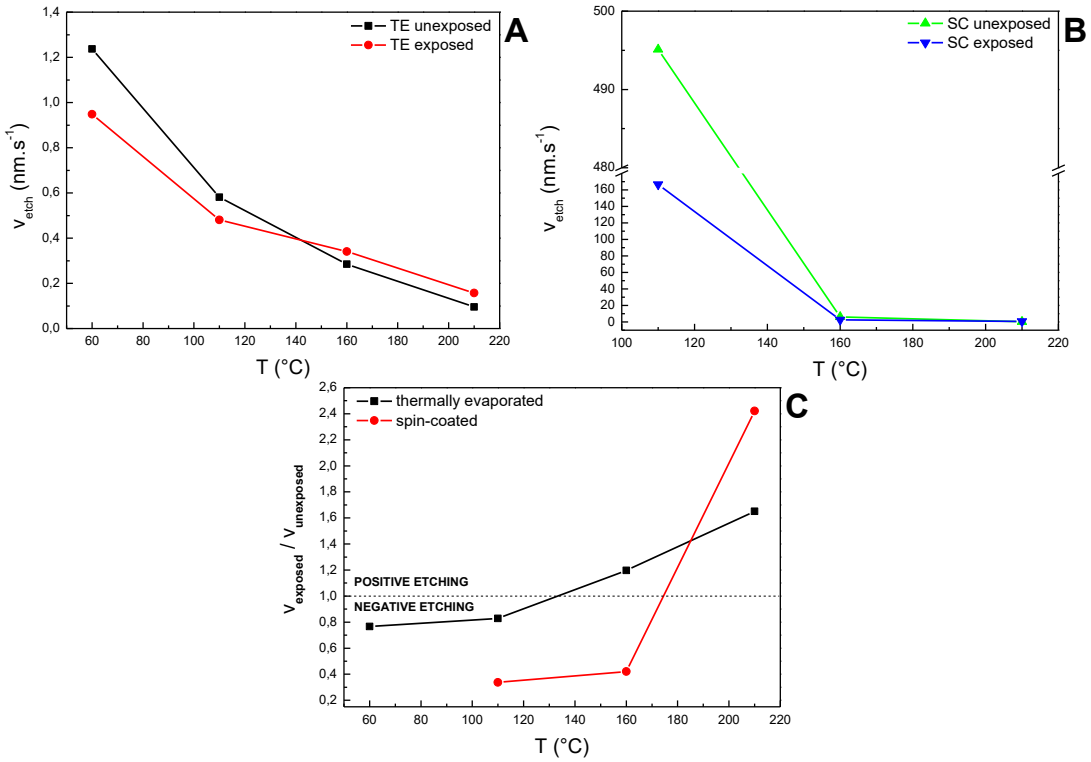

*Fig. 7. The etching rates of studied thermally evaporated (TE) **A** and spin-coated (SC) **B** $Ge_{20}Sb_5S_{75}$ thin films together with calculated etching selectivity **C**.*

Selected SC and TE $Ge_{20}Sb_5S_{75}$ thin films were structured using UV photolithography. The SC samples annealed at 160 and 210 °C were chosen with respect to their higher chemical stability and inversed etching selectivity. The TE as-prepared thin film and thin film annealed at 210 °C were chosen due to the maximum difference in their etching selectivity. The samples were exposed to UV lamp in Ar atmosphere (main peak wavelength 365 nm) through chromium grating mask with 20 μm period. Based on the etching selectivity data (Figure 7-C) the samples were etched in BA based solution for the time needed to complete dissolution of unexposed (as-prepared TE sample, SC sample annealed at 160°C) or UV exposed (TE and SC samples annealed at 210°C) thin film with the corresponding thermal treatment.

Obtained gratings were studied by AFM and SEM techniques. The SEM scans and AFM cross-sections of SC thin films (Figure 8) prove that prepared gratings have regular nearly sinusoidal profile with 20 μm grating period. The depth of grating in surface of SC samples annealed at 160 °C is ~105 nm and annealed at 210 °C is ~75 nm. The positively etched and chemically more stable SC sample annealed at 210 °C have significantly smoother surface than negatively etched SC sample annealed at 160 °C. Contrary, both obtained TE gratings prepared by photolithography have a very low quality with high surface roughness.

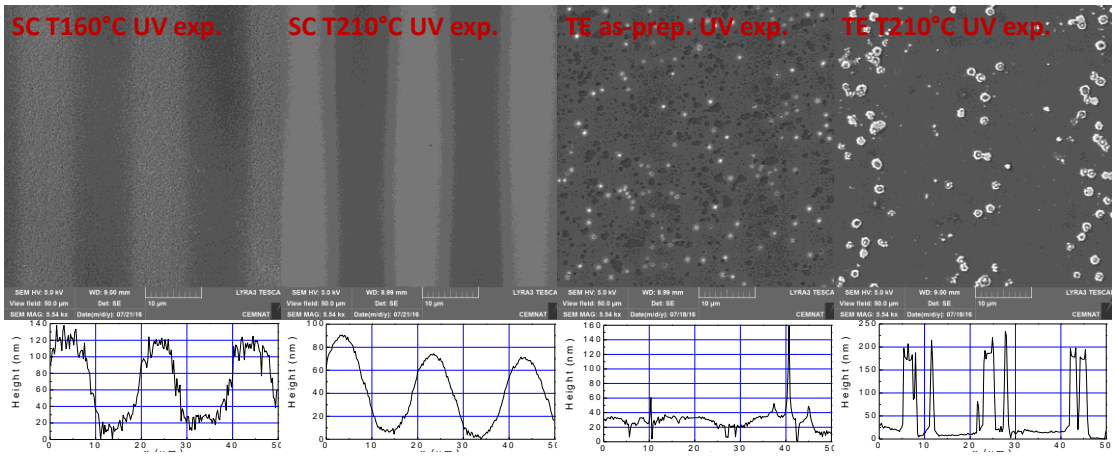

Fig. 8. SEM scans with AFM cross-sections of gratings prepared by UV photolithography (UV exp.) in surface of $Ge_{20}Sb_5S_{75}$ thin films.

To study the sensitivity of well-stabilized and chemically resistant thin films to electron beam, the SC and TE $Ge_{20}Sb_5S_{75}$ thin films annealed at 210 °C were structured by electron beam lithography (EBL). The set of two different patterns was used. The first consisted of nine 5x5 μm squares with 25 various doses ranging 100 – 2500 μC.cm^{-2} with step 100 μC.cm^{-2} (test dose structure). The second pattern was 250x250 μm grating with 5 μm period and 1000 μC.cm^{-2} dose. Thin films with latent images were etched in the BA based solution for the same time as was used for etching of samples with corresponding thermal treatment structured by UV photolithography.

The surface structures were also studied by AFM and SEM techniques. The electron beam exposed part of SC sample annealed at 210 °C was etched faster than unexposed one (positive etching). However, the material of TE thin film annealed at 210 °C was practically inert to electron beam exposure and no surface structures were obtained.

Measured depths of EBL test dose structure in surface of SC thin film annealed at 210 °C (Figure 9) demonstrate that the variation of electron beam exposure doses induces structural changes resulting in different chemical resistivity. The annealed SC sample exhibits gradual increase in depths of surface structures with dose saturation close to 1500 μC.cm^{-2}, i.e. the dose higher than 1500 μC.cm^{-2} did not cause any significant increase in their depths. Observed effect can be potentially beneficial due to the easier depth control of surface features which is useful in gray-scale pattering. Obtained linear grating (Figure 10) has regular rectangular profile with 5 μm period and relatively low surface roughness. Thus the $Ge_{20}Sb_5S_{75}$ thin films prepared by spin-coating can be successfully used for fabrication of optical micro-elements by EBL technique.

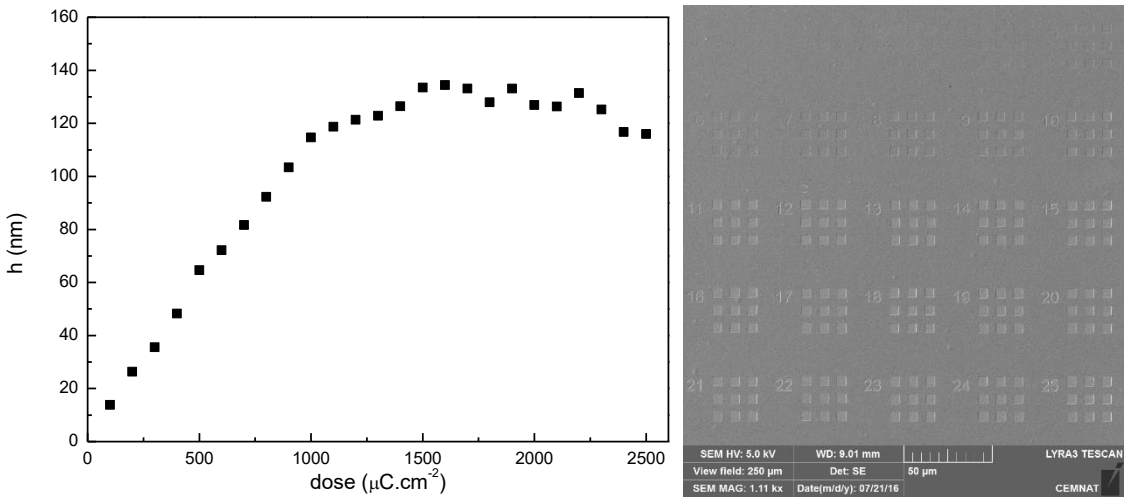

Fig. 9. The depths of EBL structured spin-coated $Ge_{20}Sb_5S_{75}$ thin film annealed at 210°C measured by AFM in dependence on exposition dose (left) and the SEM scan of EBL test dose structures (right).

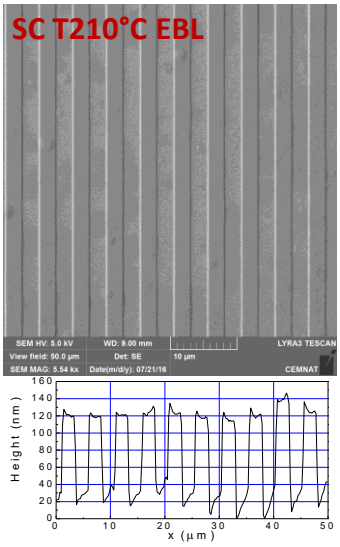

Fig. 10. SEM scan with AFM cross-section of linear gratings prepared by EBL in surface of $Ge_{20}Sb_5S_{75}$ thin films annealed at 210 °C.

Conclusion

In presented work we report on the structure and properties of non-toxic amorphous chalcogenide $Ge_{20}Sb_5S_{75}$ thin films prepared by spin-coating (SC) and thermal vacuum evaporation (TE) techniques. The influence of annealing temperature and UV exposure on structure, chemical resistance, composition and optical properties have been studied. The surface of chosen thin film samples has been additionally structured using UV photolithography and electron beam lithography.

Optical properties of studied samples have been studied by spectroscopic ellipsometry. With increasing annealing temperature, thickness of SC thin films is decreasing resulting in densification of the structure. The refractive index and optical bandgap of as-prepared SC samples are lower than the ones of TE samples, but refractive index and optical bandgap of SC samples are gradually increasing with annealing temperature. The UV exposure induced photo-

bleaching of all TE thin films and SC thin films (annealed at 110 and 160°C) and refractive index decrease of all samples have been confirmed.

Based on experimental findings from Raman spectroscopy and EDS measurements, the organic residuals in SC samples are mostly decomposed at 160°C. The annealed SC and TE thin film samples are chemically more stable with structure close to the source bulk glass. The UV exposure induced structural changes of SC samples are mainly connected with organic residuals content reduction and film compactness increase. As the annealing temperature increases, the influence of UV exposure on SC film structure and elemental composition is decreasing.

The gratings in surface of SC thin films have been successfully prepared by photolithography and electron beam lithography techniques. Due to the lower surface roughness and higher grating quality, the annealed SC samples of $Ge_{20}Sb_5S_{75}$ composition proves to be more suitable for surface structuring by both used techniques.

Acknowledgment

Authors appreciate financial support from project No. 16-13876S financed by the Grant Agency of the Czech Republic (GA CR) as well as support from the grants LM2015082 and CZ.1.05/4.1.00/11.0251 from the Ministry of Education, Youth and Sports of the Czech Republic.

References

[1] K. Tanaka, K. Shimakawa, Amorphous Chalcogenide Semiconductors and Related Materials, Springer (2011) New York.
[2] Z. Borisova, Glassy Semiconductors, Plenum Press (1981) New York.
[3] A. Galstyan, S. H. Messaddeq, V. Fortin, I. Skripachev, R. Vallée, T. Galstian, Y. Messaddeq, Opt. Mater. 47 (2015) 518–523.
[4] A. Yang, J. Qiu, M. Zhang, H. Ren, C. Zhai, S. Qi, B. Zhang, D. Tang, Z. Yang, J. Alloy Compd. 695 (2017) 1237–1242.
[5] J. Lia, X. Shen, J. Sun, K. Vu, D. Choi, R. Wang, B. Luther-Davies, S. Dai, T. Xu, Q. Nie, Thin Solid Films 545 (2013) 462–465.
[6] J. Burunkova, I. Csarnovics, I. Denisyuk, L. Daróczi, S. Kökényesi, J. Non-Cryst. Solids 402 (2014) 200–203.
[7] M. S. El-Bana, R. Bohdan, S.S. Fouad, J. Alloy Compd. 686 (2016) 115–121.
[8] A. Stronski, M. Vlcek, A. Sklenar, Quant. Electron. Optoelectron. 3 (2000) 394–399.
[9] J. D. Musgraves, N. Carlie, J. Hu, L. Petit, A. Agarwal, L. C. Kimerling, K.A. Richardson, Acta Mater. 59 (2011) 5032–5039.
[10] G. Chern, I. Lauks, J. Appl. Phys. 53 (1982) 6979–6982.
[11] G. Chern, I. Lauks, A.R. McGhie, J. Appl. Phys. 54 (1983) 4596–4601.
[12] M. Waldmann, J. D. Musgraves, K. Richardson, C.B. Arnold, J. Mater. Chem. 22 (2012) 17848–17852.
[13] S. Slang, K. Palka, H. Jain, M. Vlcek, J. Non-Cryst. Solids 457 (2017) 135–140.
[14] S. Slang, P. Janicek, K. Palka, M. Vlcek, Opt. Mater. Express 6(6) (2016) 1973–1985.
[15] S. Song, N. Carlie, J. Boundies, L. Petit, K. Richardson, C. B. Arnold, J. Non-Cryst. Solids 355 (2009) 2272–2278.
[16] L. Tichy, H. Ticha, P. Nagels, R. Callaerts, Mater. Lett. 36 (1998) 294–298.
[17] K. Tanaka, M. Mikami, Phys. Status Solidi C 8 (2011) 2756–2760.
[18] L. Loghina, K. Palka, J. Buzek, S. Slang, M. Vlcek, J. Non-Cryst. Solids 430 (2015) 21–24.

[19] D. A. G. Bruggeman, Ann. Phys. (Leipzig) 24(7) (1935) 636–679.
[20] G. E. Jellison, F. A. Modine, Appl. Phys. Lett. 69(14) (1996) 2137–2139.
[21] G.C. Chern, I. Lauks, K.H. Norian, Thin Solid Films, 123 (1985) 289–296.
[22] A. Buroff, R. Stoycheva-Topalova, J. Non-Cryst. Solids 164–166 (1993) 1207–1210.
[23] E. Savova, V. Pamukchieva, Semicond. Sci. Technol. 12 (1997) 185–188.
[24] H. Kahnt, A. Feltz, Thin Solid Films 98 (1982) 211–214.
[25] R. Todorov, J. Tasseva, V. Lozanova, A. Lalova, Tz. Iliev, A. Paneva, Adv. Cond. Matter. Phys. 2013 (2013) 1–11.
[26] R. J. Kaiser, S. Koffel, P. Pichler, A.J. Bauer, B. Amon, L. Frey, H. Ryssel, Microelectron. Eng. 88 (2011) 499–502.
[27] P. Knotek, M. Kincl, L. Tichy, D. Arsova, Z.G. Ivanova, H. Ticha, J. Non-Cryst. Solids 356 (2010) 2850–2857.
[28] P. Knotek, L. Tichy, P. Kutalek, Thin Solid Films 594 (2015) 67–73.
[29] K. Tanaka, M. Yamaguchi, J. Non-Cryst. Solids 227–230 (1998) 757–760.
[30] H. Guo, H. Tao, Y. Zhai, S. Mao, X. Zaho, Spectrochim. Acta A 67 (2007) 1351–1356.
[31] T. Haizheng, Z. Xiujiang, J. Chengbin, J. Mol. Struct. 697 (2004) 23–27.
[32] Z. Cernosek, E. Cernoskova, L. Benes, J. Mol. Struct. 435 (1997) 193–198.
[33] L. Koudelka, M. Frumar, J. Non-Cryst. Solids 41 (1980) 171–178.
[34] L. Petit, N. Carlie, F. Adamietz, M. Couzi, V. Rodriguez, K.C. Richardson, Mater. Chem. Phys. 97 (2006) 64–70.
[35] V. Nazabal, F. Charpentier, JL. Adam, P. Nemec, H. Lhermite, ML. Brandily-Anne, J. Charrier, JP: Guin, A. Moreac, Int. J. Appl. Ceram. Technol. 8(5) (2011) 990–1000.
[36] T. Cardinal, K. A. Richardson, H. Shim, A. Schulte, R. Beatty, k. Le Foulgoc, C. Meneghini, J. F. Viens, A. Villeniuve, J. Non-Cryst. Solids 256&257 (1999) 353–360.
[37] M. Pisarcik, L. Koudelka, Mater. Chem. 7 (1982) 499–507.
[38] Z. Cernosek, J. Holubova, E. Cernoskova, A. Ruzicka, J. Non-Oxide Glas. 1(1) (2009) 38–42.